Published in final edited form as:
Neuroimage. 2012 February 15; 59(4): 3227–3242. doi:10.1016/j.neuroimage.2011.11.004.

Along-tract statistics allow for enhanced tractography analysis

John B. Colby[a,b,c], **Lindsay Soderberg**[c], **Catherine Lebel**[a,c], **Ivo D. Dinov**[a,d,e], **Paul M. Thompson**[a,b,d], and **Elizabeth R. Sowell**[a,c,f]

[a]Department of Neurology, University of California Los Angeles (UCLA), Los Angeles, CA

[b]UCLA Interdepartmental Program for Biomedical Engineering, Los Angeles, CA

[c]Developmental Cognitive Neuroimaging Laboratory, Children's Hospital Los Angeles, Los Angeles, CA

[d]UCLA Laboratory of Neuro Imaging (LONI), Los Angeles, CA

[e]UCLA Department of Statistics, Los Angeles, CA

[f]Department of Pediatrics, University of Southern California (USC), Los Angeles, CA

Abstract

Diffusion imaging tractography is a valuable tool for neuroscience researchers because it allows the generation of individualized virtual dissections of major white matter tracts in the human brain. It facilitates between-subject statistical analyses tailored to the specific anatomy of each participant. There is prominent variation in diffusion imaging metrics (e.g., fractional anisotropy, FA) *within* tracts, but most tractography studies use a "tract-averaged" approach to analysis by averaging the scalar values from the many streamline vertices in a tract dissection into a single point-spread estimate for each tract. Here we describe a complete workflow needed to conduct an *along*-tract analysis of white matter streamline tract groups. This consists of 1) A flexible MATLAB toolkit for generating along-tract data based on B-spline resampling and compilation of scalar data at different collections of vertices along the curving tract spines, and 2) Statistical analysis and rich data visualization by leveraging tools available through the R platform for statistical computing. We demonstrate the effectiveness of such an along-tract approach over the tract-averaged approach in an example analysis of 10 major white matter tracts in a single subject. We also show that these techniques easily extend to between-group analyses typically used in neuroscience applications, by conducting an along-tract analysis of differences in FA between 9 individuals with fetal alcohol spectrum disorders (FASDs) and 11 typically-developing controls. This analysis reveals localized differences between FASD and control groups that were not apparent using a tract-averaged method. Finally, to validate our approach and highlight the strength of this extensible software framework, we implement 2 other methods from the literature and leverage the existing workflow tools to conduct a comparison study.

Corresponding author: Dr. Elizabeth R. Sowell Director, Developmental Cognitive Neuroimaging Laboratory Professor of Pediatrics, Keck School of Medicine, University of Southern California Children's Hospital Los Angeles 4650 Sunset Blvd., Mailstop #130 Los Angeles, CA 90027 esowell@chla.usc.edu Phone: 323-361-7347 Fax: 323-361-7836.

The authors report no conflicts of interest.

Keywords

White matter; tractography; diffusion imaging; FASD; B-spline; along-tract

1. Introduction

Since the late 1990s, diffusion magnetic resonance imaging (MRI) tractography methods have developed into a powerful set of techniques to investigate white matter connectivity in the human brain (Basser et al., 2000; Le Bihan, 2003; Conturo et al., 1999; Jones et al., 1999; Mori et al., 1999). By generating virtual dissections of different white matter tracts for each individual, tractography has proved valuable in a variety of applications – including pre- and intra-operative mapping of fiber tracts (Duncan, 2010; Maruyama et al., 2005; Prabhu et al., 2011; Young et al., 2010), and connectivity analyses of anatomical and functional brain networks (Aron et al., 2007; Behrens et al., 2003; Bullmore and Sporns, 2009; Ramnani et al., 2004). In addition to providing information about tract geometry, tractography can provide individualized volumes of interest for the investigation of white matter microstructural *qualities* in the context of development and aging (Asato et al., 2010; Davis et al., 2009; Eluvathingal et al., 2007; Huang et al., 2006, Lebel et al., 2008b, 2010; Liston et al., 2006; Penke et al., 2010; Sala et al., 2010; Schmithorst and Yuan, 2010; Verhoeven et al., 2010; Voineskos et al., 2010), numerous diseases (Ashtari et al., 2007; Kumar et al., 2010; Kunimatsu et al., 2003, Lebel et al., 2008a; Zarei et al., 2009), and the relation of brain structure to functional, cognitive, and psychiatric differences between individuals (Boorman et al., 2007; Dougherty et al., 2007; Glenn et al., 2007; Lebel and Beaulieu, 2009; Luck et al., 2011; Schulte et al., 2010; Tsang et al., 2009). As tract dissections are personalized to each individual, and do not rely on any between-subject warping to a common template space, analogous regions can be compared between individuals even when there are large differences in brain morphology. This is valuable in clinical studies, in which patients might have gross structural brain abnormalities through alterations in neurodevelopment, or in white matter microstructure as a result of disease.

Direct voxelwise comparison of diffusion imaging data is challenging, as the high-contrast edges of diffusion imaging volumes (e.g., FA maps) make them more susceptible to small misregistration errors, as well as to anatomical variability of tract position in health and disease. Even so, traditional voxelwise brain mapping is an important complement to tractography – especially now that analysis methods have advanced beyond a generic voxel-based statistical approach to include more optimized strategies tuned specifically for the analysis of white matter and diffusion imaging data (Smith et al., 2006, 2007). Furthermore, the inherent voxel-to-voxel independence of voxelwise processing allows these methods to see beyond the type of small focal disruptions that could potentially derail the streamline tractography algorithms. In general, these voxelwise studies have been in broad agreement with their tract-based counterparts (Schmithorst and Yuan, 2010; Sullivan and Pfefferbaum, 2006; Wozniak and Lim, 2006). Additionally, they have demonstrated a remarkable degree of regional heterogeneity – even *within* a given tract – in the diffusion imaging indices and observed relationships with other variables (Barnea-Goraly et al., 2010; Bava et al., 2010; Bengtsson et al., 2005; Hsu et al., 2010; Keller and Just, 2009).

To improve the localizability in deterministic tractography, there is a growing interest in methods that can provide greater *within*-tract detail. While previous work has included efforts to examine DTI metrics along tract lengths (Corouge et al., 2006; Goodlett et al., 2008, 2009; Jones et al., 2005; O'Donnell et al., 2009; Zhu et al., 2010), as well as more generic within-tract methods that can accommodate variability along even more dimensions within tracts (Yushkevich et al., 2008; Zhang et al., 2010), it has typically been focused on

individual aspects of the along-tract workflow or specific customized applications. It remains true that the large majority of streamline tractography analyses still rely on a simpler tract-averaged methodology. Therefore, there is a need for a higher-level integrated along-tract processing workflow – for an intuitive set of tools that makes it easy for applications researchers to start incorporating along-tract detail into existing tractography analyses, while facilitating statistical analysis of these data in a general linear model (GLM) framework, visualization of raw data and statistical results, and straightforward customization of all aspects of this process. To help fill this gap in the methods landscape, in this manuscript we: 1) Describe the rationale for conducting a tractography study with enhanced within-tract detail, as it relates to common tractography applications within the neuroimaging community, 2) Lay out a straightforward workflow for conducting one type of *along*-tract analysis, which is able to attain a useful balance between accessibility and improved modeling ability, 3) Demonstrate some advantages of this approach over traditional tract-averaged methods by looking at both within-subject and between-group examples, 4) Validate this approach against existing methods, while highlighting the extensible nature of this workflow toolset, and 5) Make this generic toolset available for others to use as building blocks for their own future analyses (http://www.github.com/johncolby/along-tract-stats).

2. *Along*-tract statistics

2.1. Rationale

When standard tractography methods collapse tract groups, they yield only a single mean DTI metric and variance estimate for each tract and for each subject. This processing step ignores the potentially rich anatomical variation in diffusion imaging metrics *along* the tracts, and reduces the effectiveness of this technique. To see that this added detail exists, one can browse through an FA map, or look at a histogram of its contents. FA varies widely throughout the white matter – with very low values (below 0.2) at the transition to the gray matter of the cortex, and very high values (above 0.8) in highly coherent areas like the midline corpus callosum (Fig. 1). However, when the tract-averaged estimates of mean FA in the major white matter tracts are examined, they generally fall between 0.4 and 0.6 (with the majority between the even tighter range of 0.4 to 0.5) (Wakana et al., 2007). This suggests that a large amount of blurring is taking place in the data and that potentially interesting features are being lost. Another useful way to see the extent of within-tract variability is to overlay the scalar measure of interest (e.g., FA) onto the streamlines themselves (Fig. 2). Here again it is easy to see the amount of detail within tracts. This representation, in particular, begs the analogy to a highway system: There is a collection of roads (tracts) with different speeds (FA). While there is some variation in average speed between highways (some highways are *always* slower than others), and some interesting inferences can even be made this way (traffic might universally be worse on the way to work than at midnight), to get the most complete picture of what is happening in the system, one must consider the *within*-highway effects that can have large influences (e.g., car crashes, construction, and lane geometry can all have profound focal effects on the flow of traffic). Shifting back to the brain, there is a similarly strong neurobiological basis for within-tract variability, as the vascular (Ishii et al., 1996; Ito et al., 2005), supporting glial (Innocenti et al., 1983; Monier et al., 2006, 2007; Yeh et al., 2009), biochemical (McIntosh et al., 2008; Moghaddam and Adams, 1987; Pankonin et al., 2009; Perry et al., 1971; Stamford et al., 1984; Vasung et al., 2010; Warrington et al., 2007), and biophysical environments (Childs et al., 2007) are all found to vary throughout the interior of the brain.

Beyond true *biological* variation in white matter properties along tracts, the local disturbance of diffusion imaging parameters due to *methodological* issues is another reason that makes it attractive to analyze these properties along tracts. For example, complex fiber

geometries like crossing, kissing, and partial volume averaging in general can alter properties like FA while more direct measurements of myelin content may remain unchanged (Stikov et al., 2011). Further rationale comes from the difficulty in corroborating results across studies. For any given diffusion imaging application, it is common to find that some studies have used voxelwise methods like tract-based spatial statistics (TBSS) (Smith et al., 2007), while a different collection may have used tract-averaged streamline tractography. Comparing the two types of studies is not always straightforward, and can lead to puzzling questions, like: Where along the tract-averaged ROI is the affected region located? Is it a constant difference along the whole tract, or a more focal abnormality? How does a voxelwise cluster in the internal capsule in one study relate to a significant tract-averaged tractography finding across the corticospinal tract in another? Are the same voxels even included in both studies? Attaining a higher degree of within-tract detail in our tractography analyses may help improve the level of interoperability and comparability between tractography and voxelwise methods.

Importantly, this general approach is not meant to replace the standard tract-averaged analysis techniques, but to provide the option for additional detail. Conversely, this report is not intended to be a focused exploration of the lower-level nuances between the different resampling, point alignment, and other mathematical parameters involved. Rather, we will emphasize a high-level perspective on the broader practical considerations of applications scientists, and intend to convince the reader that by making these minor modifications to existing tractography workflows, one can map the along-tract detail in the brain and enhance a broad range of white matter tractography analyses.

2.2. Overview

We aimed to create an intuitive and flexible set of modular tools with a balance between within-tract modeling complexity and accessibility. We tapped into established computational, statistical, and visualization libraries where possible, and, where decisions on low level processing approaches or parameters were needed, we attempted to make rational “middle-of-the-road” choices. Again, the overall goal was to create an end-to-end workflow that would be a useful and flexible starting point for applications-oriented neuroscientists who would otherwise conduct a standard tract-averaged tractography analysis. In short, for a given tract group, we 1) Reorient the streamlines according to a common origin, 2) Re-parameterize the streamlines with cubic B-splines, 3) Resample the streamlines so that each has the same number of points spread evenly along its length, 4) Resample the underlying voxel volume at these new vertices, and then 5) Collapse these values across streamlines at each analogous group of vertices to obtain mean scalar estimates at many locations along the tract. This allows FA or other scalar metrics to be analyzed between subjects/groups at each collection of vertices along the length of the tract, instead of using one overall tract-averaged value.

The included toolset (http://github.com/johncolby/along-tract-stats) allows the reader to begin with their own raw streamline tract groups and proceed through all the steps necessary to perform a complete along-tract analysis (these steps are described next in section 3). These tools may be operated one by one in an exploratory interactive manner, or automated in a batch mode to streamline an entire between group analysis through to the creation of customized statistical plots like those seen in this manuscript. Available to the reader are full documentation of all processing tools, an online interactive web demonstration of along-tract methods (http://www.openprocessing.org/visuals/?visualID=25715), and online tutorials including example data to download and full example analyses (http://github.com/johncolby/along-tract-stats/wiki).

3. Processing workflow

3.1. Preprocessing

Before calculating along-tract statistics, the tract groups must be delineated. There are many available software platforms to do this. We used tract groups delineated manually for each subject in TrackVis (http://www.trackvis.org). Because these tools are modular functions written in plain text in MATLAB, this framework can be straightforwardly adapted to operate on streamline data from a variety of sources. First, a tensor or alternative diffusion model is fit to the raw data, and the resulting directionality information at each voxel is used to generate a collection of streamlines representing white matter pathways across the entire brain. This initial set of fibers must then be pared down to just the groups that comprise each tract. The means of achieving this virtual dissection can vary, and a variety of atlas-based (Lebel et al., 2008b) or more unsupervised clustering (Clayden et al., 2007; Maddah et al., 2008) approaches can be attractive options depending on the size of the dataset and other considerations. Nevertheless, for between-group comparisons with clinical populations, the gold standard remains manual ROI-based dissection by a trained experimenter according to a reliable protocol. While the following descriptions will focus on FA maps from diffusion tensor imaging (DTI) data, these techniques are more generic in nature and could be applicable in a variety of other scenarios (e.g., vertex output of other packages, higher order diffusion models, multi-streamline/probabilistic tractography algorithms, mean diffusivity maps, etc.).

3.2. Reorient streamlines

Streamlines generated using brute force tractography algorithms (such as the standard Fiber Assignment by Continuous Tracking (FACT) algorithm (Mori et al., 1999) used in TrackVis) are naïve to any sort of tract origin. For example, when streamlines are generated that will end up comprising the corticospinal tract, there is no logic to say whether the streamlines are ordered to “start” at the cortex end or the brainstem end of the tract. To proceed with the cross-sectional along-tract modeling, the streamlines in each tract group must be reoriented so that they all “start” at the same end. For some relatively linear tracts, like the corticospinal tract, this can be automated. For example, the starting end of corticospinal tract streamlines could always be chosen to be the end closest to the lowest axial slice. For other tracts, like the arcuate fasciculus, however, intersubject variation in tract position and in-scanner positioning makes this less straightforward. In these cases, some sort of in-line interactive assignment may make the most sense. For example, a tract group can “pop up” on the screen and the user can click on the end that they want to designate as the “origin”. See Table 1 for a list of the tract origin conventions used in this report.

3.3. Model streamlines with cubic B-splines

The main hurdle to conducting an *along*-tract analysis at many locations within a tract is that the number of vertices that make up a streamline can vary between streamlines and subjects. Further, the spacing of the vertices within each streamline is also variable, resulting from the way the vertices are laid down as the streamlines traverse the underlying cuboidal voxel structure. One natural option, which we use to address this issue here, is to use cubic B-splines to re-parameterize the polylines as curves (a schematic is shown in Fig. 3A,B) (Corouge et al., 2006; O’Donnell et al., 2009; Zhu et al., 2010). Fig. 3 is also useful to demonstrate that by “cross-section”, we mean a collection of analogous points across streamlines, rather than a simple two-dimensional slice plane.

3.4. Resample streamlines with constant number of vertices

Once the streamlines have been approximated using cubic B-splines, they can be resampled according to different criteria. Perhaps the most straightforward option, here we focus on an approach that resamples each streamline into the same number of vertices spread evenly along their lengths, regardless of the length of the streamlines (Fig. 3C,D). This type of method accounts for inter-streamline and inter-subject scaling, and facilitates between-subject statistical analysis by maintaining a one-to-one mapping of the vertices at each cross-section, and across streamlines and subjects.

3.5. Extract scalars and collapse cross-sectionally

The final step in compiling along-tract data is to resample the underlying scalar volume (e.g., FA map) at the new sets of streamline vertices. For each subject, these scalars are then averaged at each analogous set of vertices along the tract, to obtain cross-sectional scalar mean and variance estimates. An important note with this approach is that each vertex contributes to these mean and variance estimates. Because there is usually a higher streamline density toward the center of a tract, these values will typically be weighted to favor the cores of tracts where multiple streamlines pass through the same voxels. While this is something that may or may not be desirable, given a particular application, it is an important and interesting topic to consider when performing along-tract analysis. The spatial location of the vertices can also be averaged to obtain a single streamline that represents the mean tract geometry. This aids visualization by displaying the along-tract scalar estimates of a single subject, and statistical results of between-group analyses (see Figs. 5 and 7). Again we stress that because of the flexibility this implementation allows, our processing decisions tend towards straightforward options like this in order to allow operators to develop an intuitive understanding of the broader workflow while still facilitating their implementation of other variations on these techniques if so desired at a later time (For example, see section 4.4 for an example implementation of several other options from the literature, and O'Donnell et al. (2009) for a discussion of the variability to expect among these approaches).

3.6. Between-group statistical analysis

3.6.1. Linear mixed-effects model—With cross-sectional mean FA and variance estimates obtained at many locations along a tract, and at analogous anatomical locations in each individual, we now fit statistical models to these data. This statistical analysis and later data visualization are performed using R (http://www.r-project.org), a flexible platform that is emerging as a powerful source for neuroimaging analysis resources (Tabelow et al., 2011). A linear mixed-effects (LME) model is applied serially for each tract group (*i.e.* for each tract and hemisphere) (Pinheiro and Bates, 2000). Fixed effects include: an overall intercept, a "position" factor (dummy coding the tract cross-section indices as levels of an unordered factor), a "group" factor (*i.e.* Control or Patient), and a "group:position" interaction. A subject level random effect term is also included to explain the variance component associated with this repeated measures design. Standard analysis of variance (ANOVA) can then be used to test the significance of these sets of terms in the model. The intercept term tests whether the overall grand mean FA is different from zero, which will be true by definition since there will be no streamlines if there is no FA. The group term tests whether there is an overall effect of group membership on the FA vs. position curve (analogous to the traditional tractography analysis that tests for changes in tract-averaged mean FA). While this example uses the case of a binary covariate testing for a group difference, the general linear model (GLM) can also accommodate multilevel factors or continuous covariates. The F-test across the position terms tests whether FA is, in fact, varying within the tract. Finally, the F-test across the group:position interaction term

determines whether the effect of group on FA varies based on position. In other words, it tests for any more *focal* regions of group effects isolated to regions *along* the tract. Another option would be to use a multivariate approach; either option is valid, and the choice depends on the types of questions researchers want to ask.

3.6.2. Multiple comparisons—One consequence of choosing the serial univariate approach is that the family-wise Type 1 error rate of the individual t-tests along the tracts, if examined directly, will be inflated due to the increased number of multiple comparisons (Shaffer, 1995). To address this, we can apply permutation methods to adjust the *p*-values and control the Type 1 error. Using the test for group differences as an example, we assume there is no group effect under the null hypothesis, and therefore that the group labels are exchangeable. The group labels can then be permuted, the model fit once again, and the maximum statistic across *all* comparisons recorded. This process is repeated many times to empirically build up the distribution of the *maximum* test statistic under the null hypothesis. To determine how extreme the test statistics obtained from the model fit to the real data are, one can simply compare them to this null distribution in order to obtain *p*-values corrected for multiple comparisons (Nichols and Hayasaka, 2003; Nichols and Holmes, 2002). This same procedure can also be applied to correct the *p*-values associated with other covariates of interest (age, cognitive measures, etc.).

3.7. Visualization

3.7.1. Two dimensional (see Fig. 6)—Along-tract methods increase the amount of data that results from a tractography analysis (for example, Fig. 10 contains on the order of 200,000 data points), so it is important to consider how this expanded data structure is presented to the viewer in order to maximize the usefulness of the data for various tasks. We begin with a single panel, which displays the scalar metric plotted as a function of position along the tract, and colored according to group membership. The reader is given access to the raw data for each subject, displayed semi-transparently in the background, as well as a higher-level statistical summary like the smoothed estimate of the group mean ± 95% point-wise confidence interval. Annotations can also be overlaid to convey the results of hypothesis testing – for example, an asterisk in the corner if there is an overall offset between groups, or, if the group:position F-statistic is significant, a bar to signify which component statistical tests are significant. The natural divisions in the data by tract and hemisphere can then be used to generate a facetted display of these panels, which allows for efficient review of the *entire* dataset once the reader becomes familiar with a single panel (Tufte, 2001). The panels are placed in close context, so the researcher can quickly review differences between hemispheres and tracts, and explore multivariate patterns *across* tracts and hemispheres. Whole tract properties, like the number of streamlines, may also be displayed in adjacent panels of bar or box plots. These data can even be encoded into the main panels through other plotting aesthetics such as line width. This could be used to draw attention to individuals with many streamlines or to check if outliers have too few. Finally, it is important that the generation of these statistical graphics be automated and reproducible, to provide robustness to operator errors, and easy extensibility/portability to new datasets and applications. To achieve this, we employ an implementation of the “grammar of graphics” in R (http://had.co.nz/ggplot2), which provides a rich set of abstracted graphical language tools to generate these complex multilayered plots (Wickham, 2009; Wilkinson, 2005).

3.7.2. Three dimensional (see Fig. 7)—As a complement to the 2D statistical graphics, it is also useful to view the statistical results overlaid on the tract geometry. To do this, the mean tract geometries for all of the tract groups for a representative subject can be displayed together. However, in addition to using color to encode FA or direction, we can use it to

visualize the effect sizes and *p*-values from a statistical analysis. This may be particularly useful when comparing tractography results to voxelwise results – either from the same individuals or from other analyses reported in the literature – as it directly connects these two methods and makes it easier to corroborate results.

4. Example implementation

4.1. Data acquisition and preprocessing protocol

For the within-subject and between-group analyses below (sections 4.2 and 4.3), whole brain diffusion weighted imaging data were acquired on a 3 Tesla Siemens Trio MRI scanner. Each DTI acquisition included diffusion weighted volumes (30 directions, b=1000 s/mm^2, 240 mm field of view, 96 × 96 in-plane matrix, 55 axial slices of 2.5 mm thickness, resulting in 2.5 × 2.5 × 2.5 mm^3 isotropic voxels), and one non-diffusion-weighted volume (b=0 s/mm^2). A tensor model of diffusion was fit to these raw data, and scalar maps of FA were generated. Whole-brain brute force deterministic tractography was performed according to the FACT algorithm (Mori et al., 1999), as implemented in Diffusion Toolkit v0.6 (http://www.trackvis.org/dtk). Tracking constraints included a minimum FA threshold of 0.15 and a maximum fiber turning angle of 60 degrees. Tract groups were then manually extracted in TrackVis v0.5.1 (http://www.trackvis.org) by a trained experimenter (L.S.) according to the instructions from Wakana et al. (2007). Human subjects data were collected as part of an ongoing study that has been approved by the institutional review board at UCLA.

4.2. Within-subject analysis

To validate this along-tract approach relative to the traditional tract-averaged method, we compared the two analyses to each other for ten tracts in one healthy young adult subject. The resulting tracts were compared 1) visually, by using the streamlines obtained from manual delineation and the mean tract overlaid with average cross-sectional FA values (see Fig. 5), and 2) quantitatively, by including data from all streamlines for each tract in a simple linear model, and performing an ANOVA between the along tract model (FA as a function of an intercept term and position terms) and the tract-averaged model (FA as a function of an intercept term only). As expected, along-tract processing provided highly significant increases in the explained variance for all tracts (see Table 1).

4.3. Between-group analysis

To demonstrate how easily this approach extends to between-group analyses, we conducted a comparison between a group of children with fetal alcohol spectrum disorders (FASDs) (n=9, age=13.8±2.6 years, 4 females) and typically developing controls (n=11, age=13.2±3.1 years, 5 females). FA was analyzed along tracts bilaterally within the inferior longitudinal fasciculus (ILF) and the arcuate fasciculus (AF). The ILF was chosen because it is linear, fairly “rope-like”, robustly trackable, and exhibits some of the largest group differences between these populations (Lebel et al., 2008a). Conversely, the AF was chosen as a more challenging example because it has a nonlinear geometry and is more difficult to track. The numbers of streamlines that made up these tracts were first analyzed between groups, revealing that 1) FASD subjects had significantly fewer streamlines than controls ($t=-2.35$, df=76, $p=0.022$), and 2) The ILF has significantly more streamlines than the AF ($t=3.70$, df=76, $p=4.10\times10^{-4}$). Next, as might be typical of many neuroscience applications where the experimenter seeks to map the white matter tract abnormalities associated with a certain disease, an along-tract statistical analysis was set up to look for overall offsets in the FA vs. position curves between groups, and also to look for more localized regions of effects along the tracts (see Section 3.6.1 for a complete description). This protocol failed to reveal any overall offsets between groups, but along-tract analysis did demonstrate a significant

group:position interaction in the left inferior longitudinal fasciculus (L ILF) ($F_{29,522}=2.53$, $p=2.64\times10^{-5}$). This effect localized to a region in the posterior portion of the tract where the FASD group had significantly lower FA than the control group ($t=-3.16$, df=521, $p=0.0017$, $p=0.032$ corrected) (see bottom left panel in Fig. 6, and visualization in Fig. 7).

4.4. Toolkit extensibility

To demonstrate the strength of our toolkit's extensibility and modularity, and to further validate our approach, for comparison we implemented 2 other streamline correspondence schemes from the literature. The "Distance Map" method pre-computes the minimum Euclidean distances from all points on a voxel-like grid to the vertices of a prototype fiber geometry, and uses this information to generate a lookup table describing which regions of the grid will be mapped to which regions of the prototype (Fig. 8 shows a 2-dimensional example). If multiple fibers share the same prototype (i.e., they are part of the same tract group, or different subjects' tract groups that have been registered to the same space), this has the advantage of dramatically speeding up the processing (Maddah et al., 2008). In a related "Optimal Point" matching approach, only the components of the Euclidean distances tangent to the prototype fiber geometry are considered, and matches are assigned via global cost optimization. This has the effect of strongly favoring matches that lie orthogonal to the prototype fiber (O'Donnell et al., 2009).

A plug-in was generated with these algorithms, and their alternate correspondence labels were easily incorporated into our existing data structure. Leveraging our tools already available to the user, facetted multi-panel figures of streamline correspondence plots (Fig. 9) and along-tract data plots (Fig. 10) were then generated to allow for comparison of these different methods for 3 different example tracts.

5. Discussion

5.1. Processing workflow

The main goal of this work was to generate a simple, flexible end-to-end workflow for along-tract processing and statistical analysis. We focused on the portion of the within-tract variability that exists along tracts because: 1) Previous studies show that the largest component of the within-tract variability exists along this axis, and 2) Tract groups already have longitudinal structure built in, due to the connectivity of adjacent vertices in each streamline. Clearly this decision is more appropriate for some tract geometries than others, and suggests that these methods are best suited for tract dissections that are relatively long (there is less benefit to analyzing differences along a tract if the tract is so short that there is little change along its length) and restricted to relatively tube-like point-to-point trajectories between functional or anatomical regions. For example, an analysis of the corticospinal tract's projections from the primary motor cortex would be more appropriate than an analysis that includes the fanning geometry of the *entire* corticospinal tract. Whether the assumption of radial uniformity is valid is also somewhat operator dependent, and will vary based on the types of hypotheses and effect sizes expected in the data.

We used a "constant number of vertices" approach to resample streamlines because it is simple; it implicitly scales all streamlines to the same length, controlling for variation in tract length between streamlines and subjects, and providing a natural tract "origin" at either end of the tract; and it allows straightforward between-group analysis because every subject's tract data will have a one-to-one mapping along the curved spine of this "position" axis. Although the optimal number of resampling points is expected to vary by many factors including spatial resolution, the smoothness of the changes in FA values, length of tracts, and the extent of expected group differences, a useful rule of thumb might be to resample

approximately once per voxel. Therefore, for 2.5 mm isotropic data, and a tract that averages 100 mm in length across subjects, we would resample at 40 locations along its length.

The major assumption in doing this, however, is that the ends of all the streamlines – and the vertices that make up the collection at each cross-section – are analogous to each other and therefore appropriate to lump together during statistical comparisons. Radial variability goes against this assumption, but, as previously discussed, this is relatively minor compared to the longitudinal variability. This assumption may also be less valid towards the ends of a tract group, where the individual streamlines can stray to different terminal areas, for example in the corticospinal tract, where most streamlines terminate in the lowest slice of the brainstem, but the most inferior cross-section will also include the final vertices of a few streamlines that strayed posteriorly into the cerebellum. However, with many streamlines making up each tract (approximately 100 per tract on average in our sample analysis), a few spurious fibers are unlikely to have much impact on individual subjects' along-tract estimates. Nevertheless, these issues should always be considered during statistical analysis, as varying noise levels between groups can alter their power to detect effects, and thus potentially lead to spurious conclusions. So far we have described an approach with higher *sensitivity*, which might be a useful way to explore near-cortical white matter at the expense of higher variability in the observations. Alternatively, for an approach with higher *specificity*, one could apply the same workflow we have described, but limit the analysis to more specific portions of the tract. This could be performed by extracting a subsection of the tract during delineation, subjecting the streamlines to additional constraints (length filters, uncertainty measures, etc.), or by restricting the along-tract analysis to only the high confidence central portions of tracts.

In spite of these shortcomings, this assumption of cross-sectional uniformity is more appropriate than assuming that *all* the vertices in the *entire* tract are analogous and comparable – as is the case with the tract-averaged approach. It is also important to note that this is more of a registration issue, and would still need to be considered carefully with more complex within-tract methods that might look at shape metrics or the tensor fields themselves. Indeed, even though tractography can circumvent some of the issues of traditional voxelwise registration – since the tract groups are individualized dissections based on the white matter anatomy of each subject – on some level you are still going to have to make the assumption that what you are trying to compare between individuals *should* actually be compared.

5.2. Other along-tract approaches

Instead of pinning the streamlines together at either end, another resampling strategy is to pin them down at some place in the middle of the tract. This is the approach taken by Corouge et al. (2006), where a manually identified slice plane is used to prescribe corresponding origins across streamlines somewhere in the middle of the tract where there is presumably higher confidence. While this might be advantageous for some tract geometries (In Fig. 11, panel D appears more appropriate than panel B because it avoids the partial-volume-like averaging of possibly different vertex populations towards the ends of the streamlines), it might be less appropriate for others (In Fig. 11, panel A appears more appropriate than panel C because it maintains the correspondence of vertices according to the angular geometry of the tract). This also becomes challenging for between-subject statistical analysis, given that between-subject scaling must be implemented, and there are issues of how to deal with differing numbers of vertices between streamlines and subjects (Corouge et al., 2006). To address the issue of differing tract scale among individuals when parameterizing by arc length, others have used deformable registration to bring individual subjects' tract shapes into alignment with atlas-based templates, removing shape variability while still allowing a type of along-tract parameterization (Goodlett et al., 2008). However,

since the sample locations along the streamlines are still given by a continuous arc length variable (albeit now a *standardized* arc length) there is a remaining correspondence issue since there is not a one-to-one mapping of vertices across streamlines and subjects. One progressive approach to circumvent this challenge has been to model the underlying continuous biological variation in FA *directly* though a higher dimensional framework for statistical inference called functional data analysis (Goodlett et al., 2008, 2009; Zhu et al., 2010, 2011). A simpler general approach, which has also been successful, only considers a more proximal set of vertices that have arc-length positional correspondence across all streamlines. This correspondence has variably been determined by 1) moving outwards with constant spacing from some central origin as shown in Fig. 11C,D, or 2) updating the group of corresponding vertices at each point along a mean (or otherwise prototypical) fiber geometry by considering the Euclidean distance of fiber points to each point on the prototype (Maddah et al., 2008) or other optimized cost metrics (O'Donnell et al., 2009). While these methods provide specificity, they sacrifice sensitivity to effects in the more distal regions of the longer streamlines that are effectively ignored. To gain access to these more variable (but possibly interesting) regions, an alternative approach is to group all of the continuous arc length positions into a set of discrete bins, which can then be analyzed as a factor-coded variable (Madden et al., 2009a, 2009b; O'Donnell et al., 2009). As a default option, we make available a somewhat hybrid approach in our package: an extra tie-down origin can be implemented in the middle of the tract by 1) determining the mean tract geometry (see Section 3.5), 2) assigning correspondence to the vertex in each streamline that is closest to the midpoint of this mean tract geometry, and 3) resampling the streamlines with a constant number of vertices, and with an equal proportion lying on either side of the tract midpoint. This allows for the prescription of an interior correspondence point, as suggested by Corouge et al. (2006), but does so in a way that is fully automated and avoids the extra resampling step associated with re-binning an already-interpolated arc length paramterization. Further, this approach utilizes information provided by a kind of prototypical fiber geometry (Maddah et al., 2008; O'Donnell et al., 2009), but does so in a way that still retains sensitivity to the most distal parts of the tract groups. Fig. 9A shows the evolution of this correspondence scheme as an example corticospinal tract fiber group progresses through the along-tract processing workflow. These "correspondence plots", in the efficient standardized style of O'Donnell et al. (2009), use color to show precisely which vertices will be grouped together and compared in the final analysis. This can be helpful to users of the along-tract workflow by explicitly demonstrating the effects that various processing choices have on the point alignment and correspondence scheme of their own tract groups.

To maintain balance between accessibility and modeling complexity, we employed the "constant number of vertices" resampling strategy. However, because this workflow is open source and modular, one has this flexibility to easily incorporate other variations on the individual processing components into these broader themes. For instance, consider the intuitive techniques of using functional Brodmann area masks (Oh et al., 2009) or the "bend" in the arcuate fasciculus (Yeatman et al., 2011) to prescribe additional points of correspondence across streamlines. These approaches could be easily utilized through the current framework, while retaining the advantages of fiber-tracking software interoperability, automation across multiple subjects and tract files, and rich analysis and visualization facilities. For a more *sensitive* style, the user can input the full tract groups, while for a highly *specific* style, the user can prescribe an additional interior origin, and choose to clip their tract groups using the "cut" strategy. To demonstrate the extensibility of our workflow, and further validate our hybrid resampling scheme against existing methods, we also implemented the "Distance Map" (Maddah et al., 2008) and "Optimal Point" (O'Donnell et al., 2009) correspondence schemes from the literature. By integrating these alternate algorithms in the context of the generalized along-tract workflow described in this

report, the user is given immediate access the tools that are already available for existing methods. For example, we showed how this could be used to generate faceted figures of correspondence plots (Fig. 9), as well as fully-automated, richly detailed, along-tract plots of the extracted data (Fig. 10). This is not meant as an exhaustive exploration of these different options, as there will be some variation in the data extracted by these methods as their different parameters are adjusted. Rather, this comparison shows that all methods are generally successful at extracting along-tract data from tractography fiber groups, and all benefit from being implemented in a broader along-tract workflow.

5.3. Example analyses

It is clear from applying these along-tract methods to example data that they offer promising advantages for many tractography applications. Rather than treating each tract as homogenous, these methods reveal significant along-tract variations in FA for all of the major white matter tracts studied, as would be expected based on previous voxel-based studies of the white matter (Schmithorst and Yuan, 2010; Wozniak and Lim, 2006), and other tract-based approaches that have examined FA within tracts (Concha et al., 2010; Davis et al., 2009; Sullivan and Pfefferbaum, 2006; Xue et al., 1999; Yushkevich et al., 2008). The largest benefits of shifting to an along-tract analysis are seen in the subset of tracts that are long and fairly rope-like (Fig. 5), including the corticospinal tract, the inferior fronto-occipital fasciculus, and the occipital projections of the corpus callosum (*i.e.*, the *forceps major*). Here, along-tract modeling gives a large improvement in detail and a prominent decrease in the residual unexplained variance components (e.g., in the corticospinal tract, the tract-averaged standard deviation of 0.16 decreases to less than 0.08 at many of the along-tract cross-sections). This also suggests that along-tract methods may be useful in graph-theory-type structural brain network studies, as these analyses typically employ the type of small, sometimes distant, tracking ROIs that may benefit most from this approach (Bullmore and Sporns, 2009; Hagmann et al., 2010). Further, in these analyses we commonly scale the number of streamlines between two ROIs by some measure of their quality – like average FA or inverse diffusivity – in order to investigate interesting network properties like efficiency (Rubinov and Sporns, 2010). Along-tract methods may be able to contribute to such studies by allowing for their extension to investigate focal along-tract hypotheses that are born out of an initial network analysis.

Another benefit of along-tract methods is that they can be used to address some types of partial volume effects by implementing quality control measures to check the along-tract streamline distribution for outliers or multiple streamline populations. For example, the symmetric parasagittal dips in FA in the *forceps major* likely result from partial volume averaging with cerebrospinal fluid in the adjacent lateral ventricles (Jones et al., 2005). Similarly, along-tract techniques might also be used to highlight crossing fibers areas that are not resolved by the single tensor model of diffusion.

The example between-group analysis demonstrates the richness with which these methods allow one to interrogate their data (Fig. 6). The finding of decreased FA in the inferior longitudinal fasciculus of the FASD group is particularly useful to demonstrate the advantages of modeling diffusion indices along tracts, as the effect is rather localized to only a portion of the entire tract. Although this effect region might generate a significant tract-averaged finding with enough subjects, it could easily be missed if the study were not sufficiently powered, or if there were intermingled effects in the opposite direction. Thus, the along-tract analysis increases power to detect these more focal effects, and also provides better ability to *localize* effects. For example, in regards to fetal alcohol exposure, an along-tract finding in this part of the ILF is consistent with a previous tract-averaged finding in the same tract (Lebel et al., 2008a), but is also consistent with previous voxelwise findings of decreased FA in FASD subjects in the posterior temporal lobe (Sowell et al., 2008). This

simple meta-analytical comparison becomes more meaningful with the addition of within-tract detail, as previously it might have been ambiguous whether similar effects reported in a tractography study and a voxelwise study were actually localized to similar regions.

5.4. Other options for improving within-tract tractography detail

5.4.1. Segmentation of fiber tracts—Segmentation is perhaps the simplest method to achieve greater within-tract detail, but has also had some of the broadest impact because of its easy implementation and long history of effectiveness in T1-weighted anatomical analyses. The prototypical example of this approach is an analysis of the midline corpus callosum, where it is segmented into different sub-regions that are analyzed individually. These segmentations may be generated, for example, by straightforward coronal slice planes (Wozniak et al., 2009), but have also been created by a variety of other strategies. Even before the widespread adoption of diffusion imaging, this general approach allowed for regional summaries to be generated of voxelwise and morphological analyses (e.g., (Riley et al., 1995; Thompson et al., 2000)). More recently, segmented tractography analyses have been attained in a similar manner by employing sets of masks to extract tract groups that originate from different anatomical portions of the corpus callosum (Schulte et al., 2010), or alternatively, project to different functional regions of the cortex (Huang et al., 2005; Lebel et al., 2010; Whitford et al., 2010). In an interesting variation on this theme, a prescribed structural or functional segmentation of the streamlines at one tract terminus can even be used to drive a connectivity-based segmentation of the structures that lie at the opposite tract terminus (Behrens et al., 2003). Compared to the types of methods described in this report that focus on the *along*-streamline variance component, this approach is typically implemented as a way to model the *between*-streamline variance component without having to resort to a more comprehensive within-tract framework (Yushkevich et al., 2008; Zhang et al., 2010).

5.4.2. Tract-based masks for voxelwise analysis—Instead of using different voxelwise landmarks to restrict the tractography, as described in the previous section, the process can be performed in a somewhat inverse manner, with the tract groups used to mask a voxelwise analysis, either voxel-by-voxel within the tract group mask, or collapsed along a single anatomical axis. This latter approach, in particular, is a close relative of the along-tract methods described here, and reveals some of the along-tract variation, particularly for relatively linear tracts that parallel one of the anatomical axes (e.g., the corticospinal tract) (Pfefferbaum et al., 2005; Sullivan and Pfefferbaum, 2006; Wakana et al., 2007; Xue et al., 1999). However, for tracts with more complex geometries that don't align linearly along one of these axes (e.g., the *forceps major/minor*, arcuate fasciculus, etc.), along-tract parameterization like we have described is needed to uncover these variations.

5.4.3. Shape analysis—Building on the long history of surface-based anatomical analyses of T1-weighted data (Fischl and Dale, 2000; Luders et al., 2004; Sowell et al., 2003), the *shapes* of the white matter tracts can provide important complementary information to the voxelwise intensity values that lie within the tract groups. Shape information can be used to drive a registration algorithm, bringing voxelwise (Eckstein et al., 2009) or deterministic/probabilistic-based tract groups into alignment with a common template model (Clayden et al., 2007), and allowing voxelwise analysis of intensity values throughout their interior, or projection of these values onto the shape-based tract model and subsequent surface-based analysis. Compared to the simpler spline-based along-tract strategies, which assume cross-sectional symmetry along the tracts, these more generic within-tract methods capture variability along more dimensions within a tract (Yushkevich et al., 2008; Zhang et al., 2010). While this might not be an important distinction for the long rope-like tract groups that are typical of tract dissections towards distinct functional

areas (e.g., the corticospinal tract projections to the *primary motor cortex*), it could be particularly valuable as a way to investigate variability across related bundles (e.g., the *entire* fanning geometry of the corticospinal tract, or the *entire* set of fibers that pass anywhere through the corpus callosum). An alternative approach to utilize shape information is to directly analyze the shape properties, for example, the vertex-wise deformation needed to bring each tract group shape into register (Qiu et al., 2010), the shape "context" contributed by analyzing where a set of streamlines travel beyond a voxel of interest (Adluru et al., 2009), or streamline curvature and torsion (Batchelor et al., 2006). In the context of the present report, these types of metrics can be mapped to the vertex-wise tract locations to provide complementary information to FA. For instance, the relative size (*i.e.* width) of the tract along its path could be directly calculated from the spatial spread of the vertices at each cross-section. While lacking a framework for inference, early work by Jones et al. (2005) to map alternative diffusion tensor indices and fiber orientation uncertainty *along* tracts demonstrated the rich potential of pursuing such integration.

5.4.4. Directionality-aware registration—A final class of advanced methods incorporate some sort of directionality information to drive the registration of the voxel-wise diffusion imaging data. This has been performed by developing methods to process the diffusion tensors (Alexander et al., 2001; Arsigny et al., 2006; Corouge et al., 2006; Yeo et al., 2009; Zhang et al., 2006) or the higher order orientation distribution function (ODF) representations of high angular resolution diffusion imaging (HARDI) reconstruction schemes (Chiang et al., 2008), but has also been achieved by either splitting the tensor data into multiple channels (Park et al., 2003), or summarizing the tensor data in single metrics that can be incorporated into the cost functions of existing registration algorithms in a simpler manner (Yap et al., 2009).

5.5. Relation to other diffusion models

While this report has focused on example data from a clinical-type DTI sequence (30 directions, 2.5 mm isotropic voxels) analyzed with the FACT algorithm, the general principles can extend to a variety of other diffusion models and tractography approaches that can similarly result in an analogous set of polyline-based tract groups, and their utility is likely to grow with advancements that continue to increase the effective resolution of diffusion imaging data, as this will only further highlight the within-tract heterogeneity. Similarly, these analysis tools are equally relevant to the study of additional diffusion imaging indices like mean diffusivity or axial and radial diffusion components. Other types of data could also be integrated – for example, maps could be generated showing where frontal lobe measures of executive functioning correlate with diffusion imaging indices along tracts leading from the frontal lobe. Perhaps most interesting, other types of imaging data could even be mapped to these same anatomical locations in a multi-modal approach that could examine correlations between along-tract estimates of diffusion imaging indices, and things like local shape attributes, adjacent cortical thickness, sulcal depth, or even fMRI activation indices.

6. Conclusion

It is clear from inspection of deterministic tractography dissections that there are prominent variations in scalar diffusion imaging metrics (like FA) within the major white matter tracts in the human brain. However, the majority of diffusion tractography analyses still rely on a whole-tract-averaged approach for analyzing differences in these scalar metrics. Moreover, despite excellent work on individual topics related to along-tract processing, and promising advancements towards even more exotic forms of statistical inference in this arena, this present work provides the first extensible end-to-end along-tract workflow for performing

and robustly visualizing a standard multiple regression GLM analysis, and an accompanying primer focused on practical considerations for applications-oriented scientists and clinicians. By assuming tracts are relatively tube-like structures with cross-sectional uniformity, we have implemented a straightforward spline-based resampling strategy that captures the large portion of within-tract variance that exists *along* the tracts. These tools have been incorporated into an open source end-to-end workflow for along-tract analysis, and are important because they: 1) Easily integrate into existing tractography studies, 2) Reveal a much richer data landscape than what is typically utilized by traditional tractography methods, 3) Directly extend to enable flexible between-group statistical analyses, and 4) Offer the opportunity to enhance the connectivity analyses of a wide range of neuroscience applications.

Acknowledgments

This work was performed in conjunction with the Collaborative Initiative on Fetal Alcohol Spectrum Disorders (CIFASD), which is funded by grants from the National Institute on Alcohol and Alcohol Abuse (NIAAA). Additional information about CIFASD can be found at www.cifasd.org. This work was also supported by the following organizations: National Institute of Child Health and Human Development (NICHD; R01 HD053893), National Center for Research Resources (NCRR; U54 RR021813, P41 RR013642), National Institute of General Medical Sciences (NIGMS; T32 GM008042), National Institute on Drug Abuse (NIDA; R01 DA017830, R90 DA023422), National Institute on Alcohol Abuse and Alcoholism (NIAAA; U01 AA017122, F30 AA020431), National Institute of Mental Health (NIMH; R01 MH087563), and March of Dimes (6-FY2008-50). Traffic map courtesy of SigAlert, a Westwood One company (http://www.sigalert.com).

8. References

Adluru N, Hinrichs C, Chung MK, Lee J-E, Singh V, Bigler ED, Lange N, Lainhart JE, Alexander AL. Classification in DTI using shapes of white matter tracts. Conf. Proc. IEEE Eng. Med. Biol. Soc. 2009; 2009:2719–22. [PubMed: 19964040]

Alexander DC, Pierpaoli C, Basser PJ, Gee JC. Spatial transformations of diffusion tensor magnetic resonance images. IEEE Trans. Med. Imaging. 2001; 20:1131–9. [PubMed: 11700739]

Aron AR, Behrens TE, Smith S, Frank MJ, Poldrack RA. Triangulating a cognitive control network using diffusion-weighted magnetic resonance imaging (MRI) and functional MRI. J. Neurosci. 2007; 27:3743–52. [PubMed: 17409238]

Arsigny V, Fillard P, Pennec X, Ayache N. Log-Euclidean metrics for fast and simple calculus on diffusion tensors. Magn. Reson. Med. 2006; 56:411–21. [PubMed: 16788917]

Asato MR, Terwilliger R, Woo J, Luna B. White matter development in adolescence: A DTI study. Cereb. Cortex. 2010; 20:2122–31. [PubMed: 20051363]

Ashtari M, Cottone J, Ardekani BA, Cervellione K, Szeszko PR, Wu J, Chen S, Kumra S. Disruption of white matter integrity in the inferior longitudinal fasciculus in adolescents with schizophrenia as revealed by fiber tractography. Arch. Gen. Psychiatry. 2007; 64:1270–80. [PubMed: 17984396]

Barnea-Goraly N, Lotspeich LJ, Reiss AL. Similar white matter aberrations in children with autism and their unaffected siblings: a diffusion tensor imaging study using tract-based spatial statistics. Arch. Gen. Psychiatry. 2010; 67:1052–60. [PubMed: 20921121]

Basser PJ, Pajevic S, Pierpaoli C, Duda J, Aldroubi A. In vivo fiber tractography using DT-MRI data. Magn. Reson. Med. 2000; 44:625–32. [PubMed: 11025519]

Batchelor PG, Calamante F, Tournier J-D, Atkinson D, Hill DLG, Connelly A. Quantification of the shape of fiber tracts. Magn. Reson. Med. 2006; 55:894–903. [PubMed: 16526017]

Bava S, Thayer R, Jacobus J, Ward M, Jernigan TL, Tapert SF. Longitudinal characterization of white matter maturation during adolescence. Brain Res. 2010; 1327:38–46. [PubMed: 20206151]

Behrens TEJ, Johansen-Berg H, Woolrich MW, Smith SM, Wheeler-Kingshott CAM, Boulby PA, Barker GJ, Sillery EL, Sheehan K, Ciccarelli O, Thompson AJ, Brady JM, Matthews PM. Non-invasive mapping of connections between human thalamus and cortex using diffusion imaging. Nat. Neurosci. 2003; 6:750–7. [PubMed: 12808459]

Bengtsson SL, Nagy Z, Skare S, Forsman L, Forssberg H, Ullén F. Extensive piano practicing has regionally specific effects on white matter development. Nat. Neurosci. 2005; 8:1148–50. [PubMed: 16116456]

Le Bihan D. Looking into the functional architecture of the brain with diffusion MRI. Nat. Rev. Neurosci. 2003; 4:469–80. [PubMed: 12778119]

Boorman ED, O'Shea J, Sebastian C, Rushworth MFS, Johansen-Berg H. Individual differences in white-matter microstructure reflect variation in functional connectivity during choice. Curr. Biol. 2007; 17:1426–31. [PubMed: 17689962]

Bullmore E, Sporns O. Complex brain networks: graph theoretical analysis of structural and functional systems. Nat. Rev. Neurosci. 2009; 10:186–98. [PubMed: 19190637]

Chiang MC, Leow AD, Klunder AD, Dutton RA, Barysheva M, Rose SE, McMahon KL, de Zubicaray GI, Toga AW, Thompson PM. Fluid registration of diffusion tensor images using information theory. IEEE Trans. Med. Imaging. 2008; 27:442–56. [PubMed: 18390342]

Childs C, Hiltunen Y, Vidyasagar R, Kauppinen RA. Determination of regional brain temperature using proton magnetic resonance spectroscopy to assess brain-body temperature differences in healthy human subjects. Magn. Reson. Med. 2007; 57:59–66. [PubMed: 17139620]

Clayden JD, Storkey AJ, Bastin ME. A probabilistic model-based approach to consistent white matter tract segmentation. IEEE Trans. Med. Imaging. 2007; 26:1555–61. [PubMed: 18041270]

Concha L, Livy DJ, Beaulieu C, Wheatley BM, Gross DW. In vivo diffusion tensor imaging and histopathology of the fimbria-fornix in temporal lobe epilepsy. J. Neurosci. 2010; 30:996–1002. [PubMed: 20089908]

Conturo TE, Lori NF, Cull TS, Akbudak E, Snyder AZ, Shimony JS, McKinstry RC, Burton H, Raichle ME. Tracking neuronal fiber pathways in the living human brain. Proc. Natl. Acad. Sci. U.S.A. 1999; 96:10422–7. [PubMed: 10468624]

Corouge I, Fletcher PT, Joshi S, Gouttard S, Gerig G. Fiber tract-oriented statistics for quantitative diffusion tensor MRI analysis. Med. Image Anal. 2006; 10:786–98. [PubMed: 16926104]

Davis SW, Dennis NA, Buchler NG, White LE, Madden DJ, Cabeza R. Assessing the effects of age on long white matter tracts using diffusion tensor tractography. Neuroimage. 2009; 46:530–41. [PubMed: 19385018]

Dougherty RF, Ben-Shachar M, Deutsch GK, Hernandez A, Fox GR, Wandell BA. Temporal-callosal pathway diffusivity predicts phonological skills in children. Proc. Natl. Acad. Sci. U.S.A. 2007; 104:8556–8561. [PubMed: 17483487]

Duncan JS. Imaging in the surgical treatment of epilepsy. Nat. Rev. Neurol. 2010; 6:537–50. [PubMed: 20842185]

Eckstein I, Shattuck D, Stein J, McMahon K, de Zubicaray G, Wright M, Thompson P, Toga A. Active Fibers: Matching Deformable Tract Templates to Diffusion Tensor Images. Neuroimage. 2009; 47:T82–9. [PubMed: 19457360]

Eluvathingal TJ, Hasan KM, Kramer L, Fletcher JM, Ewing-Cobbs L. Quantitative diffusion tensor tractography of association and projection fibers in normally developing children and adolescents. Cereb. Cortex. 2007; 17:2760–8. [PubMed: 17307759]

Fischl B, Dale AM. Measuring the thickness of the human cerebral cortex from magnetic resonance images. Proc. Natl. Acad. Sci. U.S.A. 2000; 97:11050–5. [PubMed: 10984517]

Glenn OA, Ludeman NA, Berman JI, Wu YW, Lu Y, Bartha AI, Vigneron DB, Chung SW, Ferriero DM, Barkovich AJ, Henry RG. Diffusion tensor MR imaging tractography of the pyramidal tracts correlates with clinical motor function in children with congenital hemiparesis. AJNR Am. J. Neuroradiol. 2007; 28:1796–802. [PubMed: 17893220]

Goodlett CB, Fletcher PT, Gilmore JH, Gerig G. Group statistics of DTI fiber bundles using spatial functions of tensor measures. Med. Image Comput. Comput. Assist. Interv. 2008; 11:1068–75. [PubMed: 18979851]

Goodlett CB, Fletcher PT, Gilmore JH, Gerig G. Group analysis of DTI fiber tract statistics with application to neurodevelopment. Neuroimage. 2009; 45:S133–42. [PubMed: 19059345]

Hagmann P, Sporns O, Madan N, Cammoun L, Pienaar R, Wedeen VJ, Meuli R, Thiran J-P, Grant PE. White matter maturation reshapes structural connectivity in the late developing human brain. Proc. Natl. Acad. Sci. U.S.A. 2010; 107:19067–72. [PubMed: 20956328]

Hsu J, Hecke WV, Bai C, Lee C, Tsai Y, Chiu H, Jaw F, Hsu C, Leu J, Chen W, Leemans A. Microstructural white matter changes in normal aging: A diffusion tensor imaging study with higher-order polynomial regression models. Neuroimage. 2010; 49:32–43. [PubMed: 19699804]

Huang H, Zhang J, Jiang H, Wakana S, Poetscher L, Miller MI, van Zijl PCM, Hillis AE, Wytik R, Mori S. DTI tractography based parcellation of white matter: application to the mid-sagittal morphology of corpus callosum. Neuroimage. 2005; 26:195–205. [PubMed: 15862219]

Huang H, Zhang J, Wakana S, Zhang W, Ren T, Richards LJ, Yarowsky P, Donohue P, Graham E, van Zijl PCM, Mori S. White and gray matter development in human fetal, newborn and pediatric brains. Neuroimage. 2006; 33:27–38. [PubMed: 16905335]

Innocenti GM, Clarke S, Koppel H. Transitory macrophages in the white matter of the developing visual cortex. II. Development and relations with axonal pathways. Brain Res. 1983; 313:55–66. [PubMed: 6198052]

Ishii K, Sasaki M, Kitagaki H, Sakamoto S, Yamaji S, Maeda K. Regional difference in cerebral blood flow and oxidative metabolism in human cortex. J. Nucl. Med. 1996; 37:1086–8. [PubMed: 8965174]

Ito H, Kanno I, Fukuda H. Human cerebral circulation: positron emission tomography studies. Ann. Nucl. Med. 2005; 19:65–74. [PubMed: 15909484]

Jones DK, Simmons A, Williams SC, Horsfield MA. Non-invasive assessment of axonal fiber connectivity in the human brain via diffusion tensor MRI. Magn. Reson. Med. 1999; 42:37–41. [PubMed: 10398948]

Jones DK, Travis AR, Eden G, Pierpaoli C, Basser PJ. PASTA: pointwise assessment of streamline tractography attributes. Magn. Reson. Med. 2005; 53:1462–7. [PubMed: 15906294]

Keller TA, Just MA. Altering cortical connectivity: remediation-induced changes in the white matter of poor readers. Neuron. 2009; 64:624–31. [PubMed: 20005820]

Kumar A, Sundaram SK, Sivaswamy L, Behen ME, Makki MI, Ager J, Janisse J, Chugani HT, Chugani DC. Alterations in frontal lobe tracts and corpus callosum in young children with autism spectrum disorder. Cereb. Cortex. 2010; 20:2103–13. [PubMed: 20019145]

Kunimatsu A, Aoki S, Masutani Y, Abe O, Mori H, Ohtomo K. Three-dimensional white matter tractography by diffusion tensor imaging in ischaemic stroke involving the corticospinal tract. Neuroradiology. 2003; 45:532–5. [PubMed: 12856090]

Lebel C, Beaulieu C. Lateralization of the arcuate fasciculus from childhood to adulthood and its relation to cognitive abilities in children. Hum. Brain Mapp. 2009; 30:3563–73. [PubMed: 19365801]

Lebel C, Caverhill-Godkewitsch S, Beaulieu C. Age-related regional variations of the corpus callosum identified by diffusion tensor tractography. Neuroimage. 2010; 52:20–31. [PubMed: 20362683]

Lebel C, Rasmussen C, Wyper K, Walker L, Andrew G, Yager J, Beaulieu C. Brain diffusion abnormalities in children with fetal alcohol spectrum disorder. Alcohol. Clin. Exp. Res. 2008a; 32:1732–1740. [PubMed: 18671811]

Lebel C, Walker L, Leemans A, Phillips L, Beaulieu C. Microstructural maturation of the human brain from childhood to adulthood. Neuroimage. 2008b; 40:1044–1055. [PubMed: 18295509]

Liston C, Watts R, Tottenham N, Davidson MC, Niogi S, Ulug AM, Casey BJ. Frontostriatal microstructure modulates efficient recruitment of cognitive control. Cereb. Cortex. 2006; 16:553–60. [PubMed: 16033925]

Luck D, Buchy L, Czechowska Y, Bodnar M, Pike GB, Campbell JSW, Achim A, Malla A, Joober R, Lepage M. Fronto-temporal disconnectivity and clinical short-term outcome in first episode psychosis: A DTI-tractography study. J. Psychiatr. Res. 2011; 45:369–77. [PubMed: 20708198]

Luders E, Narr KL, Thompson PM, Rex DE, Jancke L, Steinmetz H, Toga AW. Gender differences in cortical complexity. Nat. Neurosci. 2004; 7:799–800. [PubMed: 15338563]

Maddah M, Grimson WEL, Warfield SK, Wells WM. A unified framework for clustering and quantitative analysis of white matter fiber tracts. Med. Image Anal. 2008; 12:191–202. [PubMed: 18180197]

Madden DJ, Bennett IJ, Song AW. Cerebral white matter integrity and cognitive aging: contributions from diffusion tensor imaging. Neuropsychol. Rev. 2009a; 19:415–35. [PubMed: 19705281]

Madden DJ, Spaniol J, Costello MC, Bucur B, White LE, Cabeza R, Davis SW, Dennis NA, Provenzale JM, Huettel SA. Cerebral white matter integrity mediates adult age differences in cognitive performance. J. Cogn. Neurosci. 2009b; 21:289–302. [PubMed: 18564054]

Maruyama K, Kamada K, Shin M, Itoh D, Aoki S, Masutani Y, Tago M, Kirino T. Integration of three-dimensional corticospinal tractography into treatment planning for gamma knife surgery. J. Neurosurg. 2005; 102:673–7. [PubMed: 15871510]

McIntosh AM, Moorhead TWJ, Job D, Lymer GKS, Maniega S.M. noz, McKirdy J, Sussmann JED, Baig BJ, Bastin ME, Porteous D, Evans KL, Johnstone EC, Lawrie SM, Hall J. The effects of a neuregulin 1 variant on white matter density and integrity. Mol. Psychiatry. 2008; 13:1054–9. [PubMed: 17925794]

Moghaddam B, Adams RN. Regional differences in resting extracellular potassium levels of rat brain. Brain Res. 1987; 406:337–40. [PubMed: 3567631]

Monier A, Adle-Biassette H, Delezoide A-L, Evrard P, Gressens P, Verney C. Entry and distribution of microglial cells in human embryonic and fetal cerebral cortex. J. Neuropathol. Exp. Neurol. 2007; 66:372–82. [PubMed: 17483694]

Monier A, Evrard P, Gressens P, Verney C. Distribution and differentiation of microglia in the human encephalon during the first two trimesters of gestation. J. Comp. Neurol. 2006; 499:565–82. [PubMed: 17029271]

Mori S, Crain BJ, Chacko VP, van Zijl PC. Three-dimensional tracking of axonal projections in the brain by magnetic resonance imaging. Ann. Neurol. 1999; 45:265–9. [PubMed: 9989633]

Nichols T, Hayasaka S. Controlling the familywise error rate in functional neuroimaging: a comparative review. Stat. Methods Med. Res. 2003; 12:419–46. [PubMed: 14599004]

Nichols TE, Holmes AP. Nonparametric permutation tests for functional neuroimaging: a primer with examples. Hum. Brain Mapp. 2002; 15:1–25. [PubMed: 11747097]

O'Donnell L, Westin C, Golby A. Tract-based morphometry for white matter group analysis. Neuroimage. 2009; 45:832–44. [PubMed: 19154790]

Oh JS, Kubicki M, Rosenberger G, Bouix S, Levitt JJ, McCarley RW, Westin C-F, Shenton ME. Thalamo-frontal white matter alterations in chronic schizophrenia: a quantitative diffusion tractography study. Hum. Brain Mapp. 2009; 30:3812–3825. [PubMed: 19449328]

Pankonin MS, Sohi J, Kamholz J, Loeb JA. Differential distribution of neuregulin in human brain and spinal fluid. Brain Res. 2009; 1258:1–11. [PubMed: 19150438]

Park H-J, Kubicki M, Shenton ME, Guimond A, McCarley RW, Maier SE, Kikinis R, Jolesz FA, Westin C-F. Spatial normalization of diffusion tensor MRI using multiple channels. Neuroimage. 2003; 20:1995–2009. [PubMed: 14683705]

Penke L, Maniega S.M. noz, Murray C, Gow AJ, Hernández MCV, Clayden JD, Starr JM, Wardlaw JM, Bastin ME, Deary IJ. A general factor of brain white matter integrity predicts information processing speed in healthy older people. J. Neurosci. 2010; 30:7569–74. [PubMed: 20519531]

Perry TL, Berry K, Hansen S, Diamond S, Mok C. Regional distribution of amino acids in human brain obtained at autopsy. J. Neurochem. 1971; 18:513–9. [PubMed: 5559257]

Pfefferbaum A, Adalsteinsson E, Sullivan EV. Frontal circuitry degradation marks healthy adult aging: Evidence from diffusion tensor imaging. Neuroimage. 2005; 26:891–9. [PubMed: 15955499]

Pinheiro, J.; Bates, D. Mixed-Effects Models in S and S-Plus. Springer; New York: 2000.

Prabhu SS, Gasco J, Tummala S, Weinberg JS, Rao G. Intraoperative magnetic resonance imaging-guided tractography with integrated monopolar subcortical functional mapping for resection of brain tumors. J. Neurosurg. 2011; 114:719–26. [PubMed: 20964594]

Qiu A, Oishi K, Miller MI, Lyketsos CG, Mori S, Albert M. Surface-based analysis on shape and fractional anisotropy of white matter tracts in Alzheimer's disease. PLoS ONE. 2010; 5:e9811. [PubMed: 20339558]

Ramnani N, Behrens TEJ, Penny W, Matthews PM. New approaches for exploring anatomical and functional connectivity in the human brain. Biol. Psychiatry. 2004; 56:613–9. [PubMed: 15522243]

Riley EP, Mattson SN, Sowell ER, Jernigan TL, Sobel DF, Jones KL. Abnormalities of the corpus callosum in children prenatally exposed to alcohol. Alcohol. Clin. Exp. Res. 1995; 19:1198–202. [PubMed: 8561290]

Rubinov M, Sporns O. Complex network measures of brain connectivity: Uses and interpretations. Neuroimage. 2010; 52:1059–69. [PubMed: 19819337]

Sala S, Agosta F, Pagani E, Copetti M, Comi G, Filippi M. Microstructural changes and atrophy in brain white matter tracts with aging. Neurobiol. Aging. 2010 In press.

Schmithorst V, Yuan W. White matter development during adolescence as shown by diffusion MRI. Brain Cogn. 2010; 72:16–25. [PubMed: 19628324]

Schulte T, Müller-Oehring EM, Rohlfing T, Pfefferbaum A, Sullivan EV. White matter fiber degradation attenuates hemispheric asymmetry when integrating visuomotor information. J. Neurosci. 2010; 30:12168–78. [PubMed: 20826679]

Shaffer JP. Multiple Hypothesis Testing. Annu. Rev. Psychol. 1995; 46:561–584.

Smith SM, Jenkinson M, Johansen-Berg H, Rueckert D, Nichols TE, Mackay CE, Watkins KE, Ciccarelli O, Cader MZ, Matthews PM, Behrens TEJ. Tract-based spatial statistics: voxelwise analysis of multi-subject diffusion data. Neuroimage. 2006; 31:1487–505. [PubMed: 16624579]

Smith SM, Johansen-Berg H, Jenkinson M, Rueckert D, Nichols TE, Miller KL, Robson MD, Jones DK, Klein JC, Bartsch AJ, Behrens TEJ. Acquisition and voxelwise analysis of multi-subject diffusion data with tract-based spatial statistics. Nat. Protoc. 2007; 2:499–503. [PubMed: 17406613]

Sowell ER, Johnson A, Kan E, Lu LH, Van Horn JD, Toga AW, O'Connor MJ, Bookheimer SY. Mapping white matter integrity and neurobehavioral correlates in children with fetal alcohol spectrum disorders. J. Neurosci. 2008; 28:1313–9. [PubMed: 18256251]

Sowell ER, Peterson BS, Thompson PM, Welcome SE, Henkenius AL, Toga AW. Mapping cortical change across the human life span. Nat. Neurosci. 2003; 6:309–15. [PubMed: 12548289]

Stamford JA, Kruk ZL, Millar J. Regional differences in extracellular ascorbic acid levels in the rat brain determined by high speed cyclic voltammetry. Brain Res. 1984; 299:289–95. [PubMed: 6733451]

Stikov N, Perry LM, Mezer A, Rykhlevskaia E, Wandell BA, Pauly JM, Dougherty RF. Bound pool fractions complement diffusion measures to describe white matter micro and macrostructure. NeuroImage. 2011; 54:1112–1121. [PubMed: 20828622]

Sullivan EV, Pfefferbaum A. Diffusion tensor imaging and aging. Neurosci. Biobehav. Rev. 2006; 30:749–61. [PubMed: 16887187]

Tabelow K, Clayden JD, de Micheaux PL, Polzehl J, Schmid VJ, Whitcher B. Image analysis and statistical inference in neuroimaging with R. NeuroImage. 2011; 55:1686–1693. [PubMed: 21238596]

Thompson PM, Giedd JN, Woods RP, MacDonald D, Evans AC, Toga AW. Growth patterns in the developing brain detected by using continuum mechanical tensor maps. Nature. 2000; 404:190–3. [PubMed: 10724172]

Tsang JM, Dougherty RF, Deutsch GK, Wandell BA, Ben-Shachar M. Frontoparietal white matter diffusion properties predict mental arithmetic skills in children. Proc. Natl. Acad. Sci. U.S.A. 2009; 106:22546–22551. [PubMed: 19948963]

Tufte, ER. The Visual Display of Quantitative Information. 2nd ed. Graphics Press; Cheshire, CT: 2001.

Vasung L, Huang H, sević N. sa J-M, Pletikos M, Mori S, Kostović I. Development of axonal pathways in the human fetal fronto-limbic brain: histochemical characterization and diffusion tensor imaging. J. Anat. 2010; 217:400–17. [PubMed: 20609031]

Verhoeven JS, Sage CA, Leemans A, Hecke WV, Callaert D, Peeters R, Cock PD, Lagae L, Sunaert S. Construction of a stereotaxic DTI atlas with full diffusion tensor information for studying white matter maturation from childhood to adolescence using tractography-based segmentations. Hum. Brain Mapp. 2010; 31:470–86. [PubMed: 19957267]

Voineskos AN, Rajji TK, Lobaugh NJ, Miranda D, Shenton ME, Kennedy JL, Pollock BG, Mulsant BH. Age-related decline in white matter tract integrity and cognitive performance: A DTI tractography and structural equation modeling study. Neurobiol. Aging. 2010 In press.

Wakana S, Caprihan A, Panzenboeck MM, Fallon JH, Perry M, Gollub RL, Hua K, Zhang J, Jiang H, Dubey P, Blitz A, van Zijl P, Mori S. Reproducibility of quantitative tractography methods applied to cerebral white matter. Neuroimage. 2007; 36:630–44. [PubMed: 17481925]

Warrington NM, Woerner BM, Daginakatte GC, Dasgupta B, Perry A, Gutmann DH, Rubin JB. Spatiotemporal differences in CXCL12 expression and cyclic AMP underlie the unique pattern of optic glioma growth in neurofibromatosis type 1. Cancer Res. 2007; 67:8588–95. [PubMed: 17875698]

Whitford TJ, Kubicki M, Schneiderman JS, O'Donnell LJ, King R, Alvarado JL, Khan U, Markant D, Nestor PG, Niznikiewicz M, McCarley RW, Westin C-F, Shenton ME. Corpus callosum abnormalities and their association with psychotic symptoms in patients with schizophrenia. Biol. Psychiatry. 2010; 68:70–7. [PubMed: 20494336]

Wickham, H. ggplot2 - Elegant Graphics for Data Analysis. Springer; New York: 2009.

Wilkinson, L. The Grammar of Graphics. 2nd ed. Springer; New York: 2005.

Wozniak JR, Lim KO. Advances in white matter imaging: a review of in vivo magnetic resonance methodologies and their applicability to the study of development and aging. Neurosci. Biobehav. Rev. 2006; 30:762–74. [PubMed: 16890990]

Wozniak JR, Muetzel RL, Mueller BA, McGee CL, Freerks MA, Ward EE, Nelson ML, Chang P-N, Lim KO. Microstructural corpus callosum anomalies in children with prenatal alcohol exposure: an extension of previous diffusion tensor imaging findings. Alcohol. Clin. Exp. Res. 2009; 33:1825–35. [PubMed: 19645729]

Xue R, van Zijl PC, Crain BJ, Solaiyappan M, Mori S. In vivo three-dimensional reconstruction of rat brain axonal projections by diffusion tensor imaging. Magn. Reson. Med. 1999; 42:1123–7. [PubMed: 10571934]

Yap P-T, Wu G, Zhu H, Lin W, Shen D. TIMER: tensor image morphing for elastic registration. Neuroimage. 2009; 47:549–63. [PubMed: 19398022]

Yeatman JD, Dougherty RF, Rykhlevskaia E, Sherbondy AJ, Deutsch GK, Wandell BA, Ben-Shachar M. Anatomical Properties of the Arcuate Fasciculus Predict Phonological and Reading Skills in Children. J. Cogn. Neurosci. 2011 In press.

Yeh T-H, Lee DY, Gianino SM, Gutmann DH. Microarray analyses reveal regional astrocyte heterogeneity with implications for neurofibromatosis type 1 (NF1)-regulated glial proliferation. Glia. 2009; 57:1239–49. [PubMed: 19191334]

Yeo BTT, Vercauteren T, Fillard P, Peyrat J-M, Pennec X, Golland P, Ayache N, Clatz O. DT-REFinD: diffusion tensor registration with exact finite-strain differential. IEEE Trans. Med. Imaging. 2009; 28:1914–28. [PubMed: 19556193]

Young RJ, Brennan N, Fraser JF, Brennan C. Advanced imaging in brain tumor surgery. Neuroimaging Clin. N. Am. 2010; 20:311–35. [PubMed: 20708549]

Yushkevich PA, Zhang H, Simon TJ, Gee JC. Structure-specific statistical mapping of white matter tracts. Neuroimage. 2008; 41:448–61. [PubMed: 18407524]

Zarei M, Damoiseaux J, Morgese C, Beckmann C, Smith S, Matthews P, Scheltens P, Rombouts S, Barkhof F. Regional white matter integrity differentiates between vascular dementia and Alzheimer disease. Stroke. 2009; 40:773–9. [PubMed: 19164789]

Zhang H, Awate SP, Das SR, Woo JH, Melhem ER, Gee JC, Yushkevich PA. A tract-specific framework for white matter morphometry combining macroscopic and microscopic tract features. Med. Image Anal. 2010; 14:666–73. [PubMed: 20547469]

Zhang H, Yushkevich PA, Alexander DC, Gee JC. Deformable registration of diffusion tensor MR images with explicit orientation optimization. Med. Image Anal. 2006; 10:764–785. [PubMed: 16899392]

Zhu H, Kong L, Li R, Styner M, Gerig G, Lin W, Gilmore JH. FADTTS: Functional analysis of diffusion tensor tract statistics. NeuroImage. 2011; 56:1412–25. [PubMed: 21335092]

Zhu H, Styner M, Tang N, Liu Z, Lin W, Gilmore J. FRATS: Functional regression analysis of DTI tract statistics. IEEE Trans. Med. Imaging. 2010; 29:1039–49. [PubMed: 20335089]

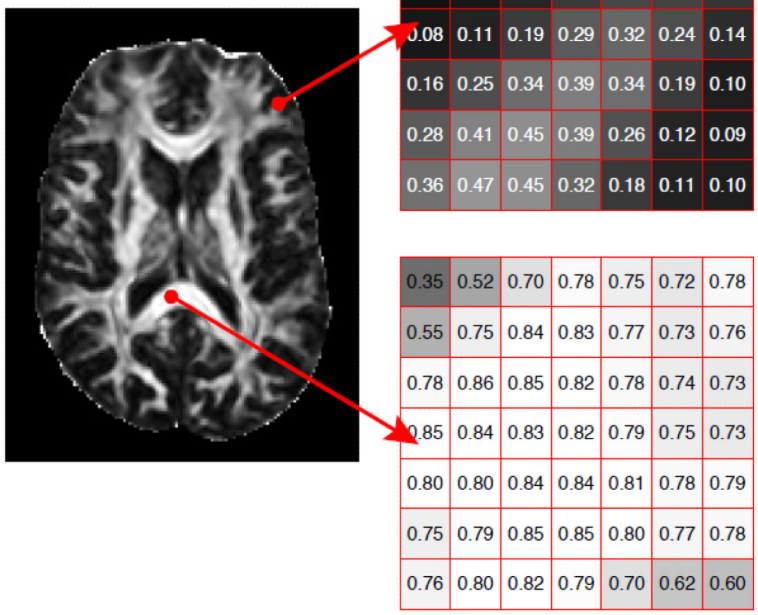

Figure 1. FA variations throughout the brain

Fractional anisotropy (FA) varies widely throughout the white matter, with values ranging from below 0.2 at the transition to gray matter near the cortex (top breakout panel), to greater than 0.8 in tightly coherent fiber bundles like the midline corpus callosum (bottom breakout panel).

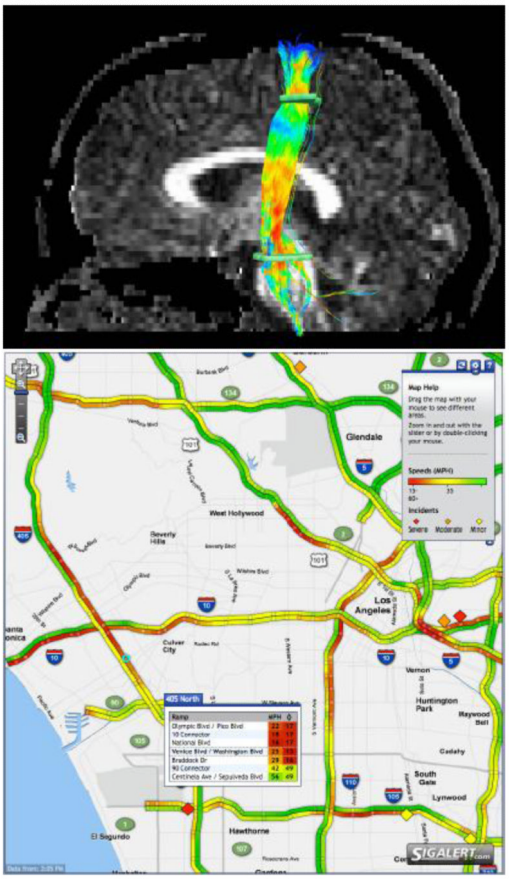

Figure 2. Along-tract variations in the human brain and the Los Angeles highway system

(Top panel) Deterministic tractography dissection of the left corticospinal tract in one individual. Color is used to encode FA variations along the tract. (Bottom panel) Highway map of Los Angeles, CA. Color is used to encode traffic speed.

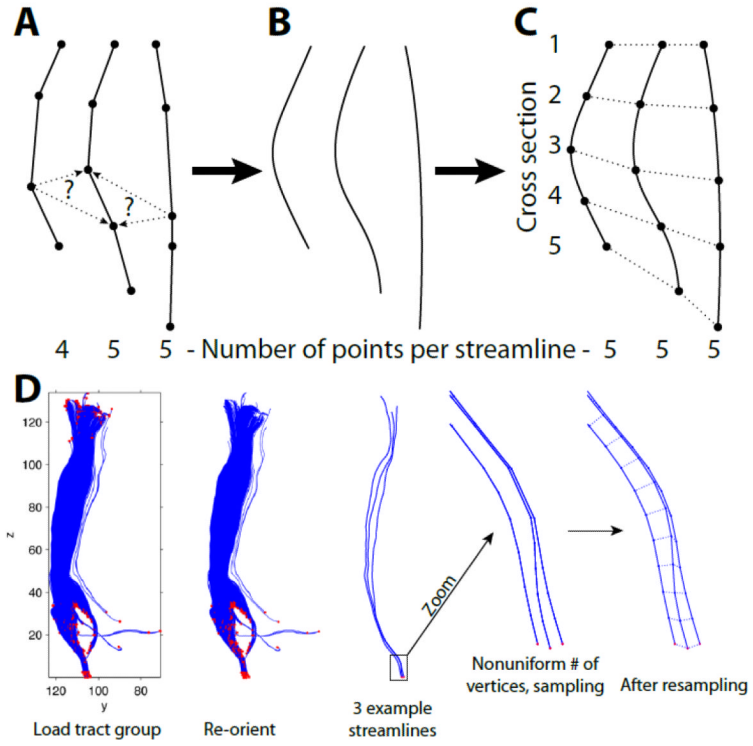

Figure 3. B-spline based resampling

(A) Raw deterministic tractography streamlines are difficult to analyze along their length due to differing numbers of vertices, and non-uniform spatial sampling. To address this, the raw streamlines can be re-parameterized using cubic B-spline curves (B), and then resampled to allow for a straightforward analysis at different tract "cross-sections" (C). (D) Streamline processing for an example tract group (left corticospinal tract) derived from actual data. The streamlines are first reoriented so that their origins (red points) are near a common tract terminus, and then resampled to allow for comparison across streamlines at different cross-sections (dotted lines, right).

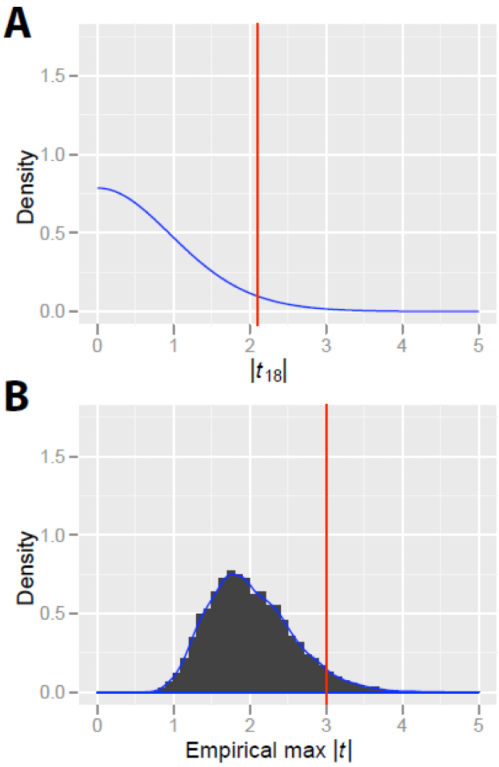

Figure 4. Correcting for multiple comparisons

(A) Theoretical probability density function and $p<0.05$ critical value for a single two-tailed *t*-test with 18 degrees of freedom. (B) The empirical null distribution of the *maximum* test statistic across the many along-tract comparisons from an example analysis. The $p<0.05$ critical value has been shifted appropriately to control the family-wise error rate (*i.e.* the chance of *any* false positives across *all* of the multiple comparisons).

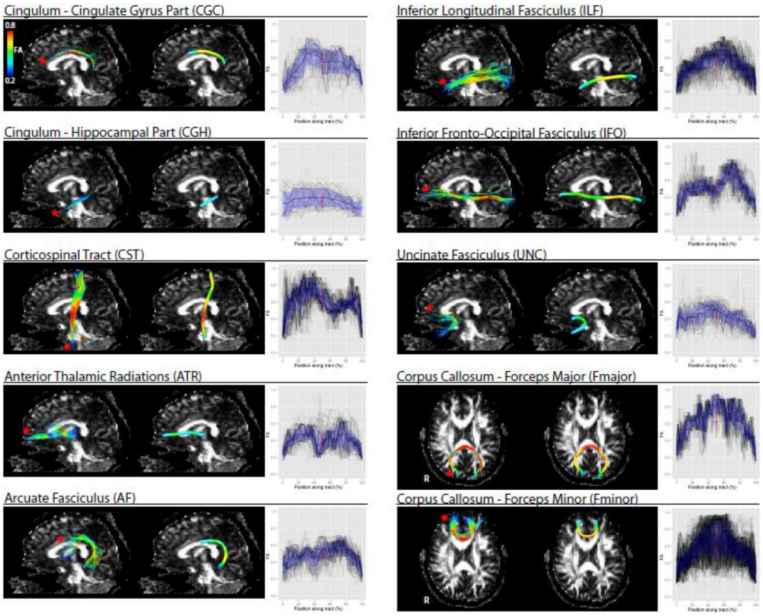

Figure 5. Single subject along-tract analysis

The raw streamlines (left panels), mean tract geometries (middle panels), and along-tract variations in FA (right panels) are displayed for 10 major white matter tracts in the human brain. In the two streamline views, color is used to encode variation in FA. In the along-tract plots, FA is plotted versus position from tract origin (designated as the side of the tract near the red star in the streamline views; see also Table 1). The distribution of individual streamlines is shown in the background (black lines; transparency and slight x-axis jitter used to control overplotting). Overlaid is the along-tract cross-sectional mean FA (blue; ± pointwise standard deviation). Also included is the standard tract-averaged point-spread estimate (red).

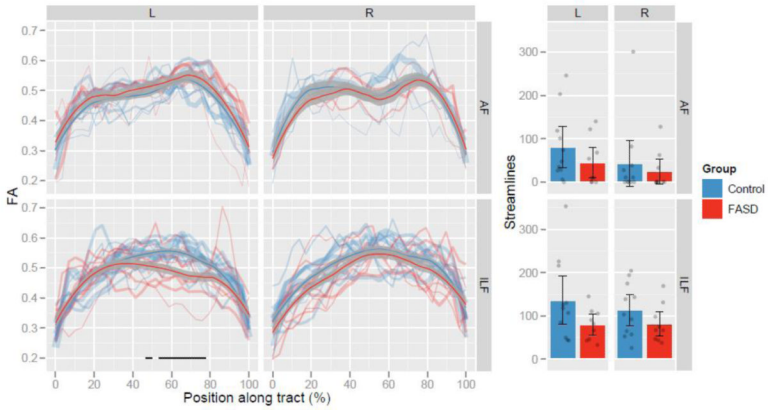

Figure 6. Between-group along-tract analysis in fetal alcohol exposure

FA is plotted versus position from tract origin, with plots faceted by tract name and hemisphere, and colored according to group membership (Control or FASD). Along-tract estimates from individual subjects are displayed semi-transparently in the background (line width encodes the relative number of streamlines), and are overlaid with locally weighted smooth estimates of the group means (± pointwise 95% confidence range). The number of streamlines in each tract (± pointwise 95% confidence interval) is also included in an accompanying panel at right.

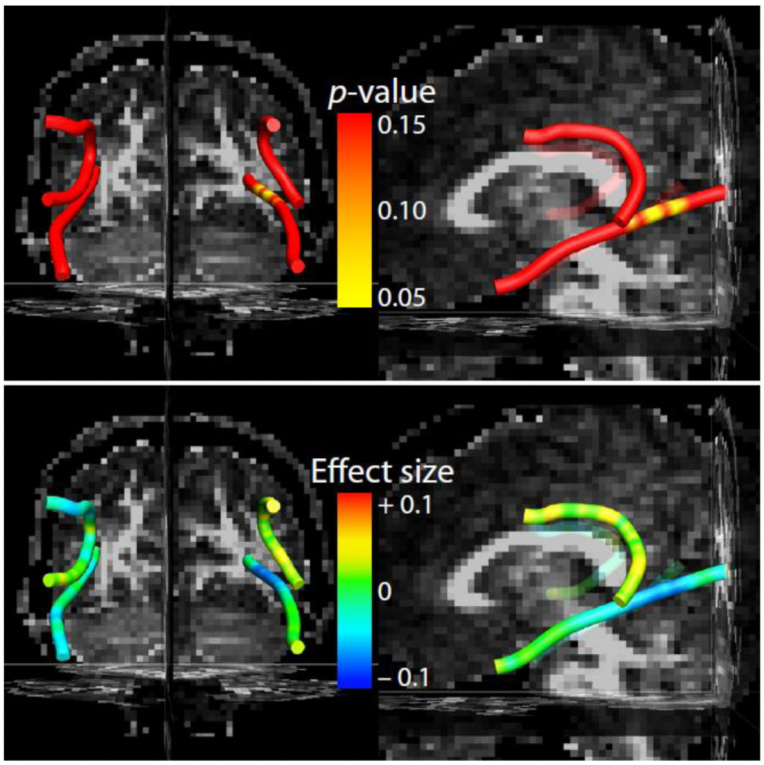

Figure 7. Visualization of between-group results

Statistical results are displayed on the mean tract geometry of one representative subject. (A) *p*-value map (yellow color indicates regions of significant effects ($p<0.05$, corrected). (B) Effect size map (cooler colors represent regions of decreased FA in FASD subjects).

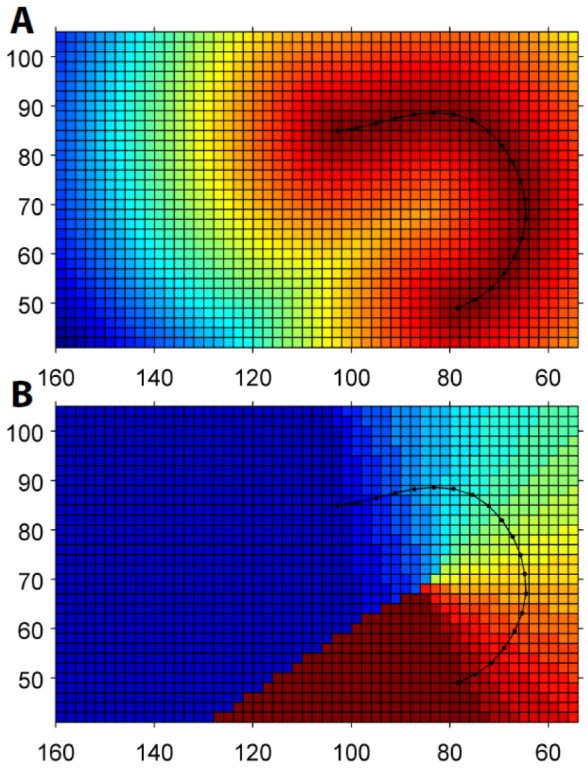

Figure 8. Distance map method (2-dimensional)

Euclidean distances are calculated from each point on a grid to each point on the prototype fiber, and used to generate a minimum distance map (A) and corresponding label map (B) matching regions of the grid to different points on the prototype. This lookup table can then be used for rapid processing of multiple fibers that share the same prototype (Maddah et al., 2008).

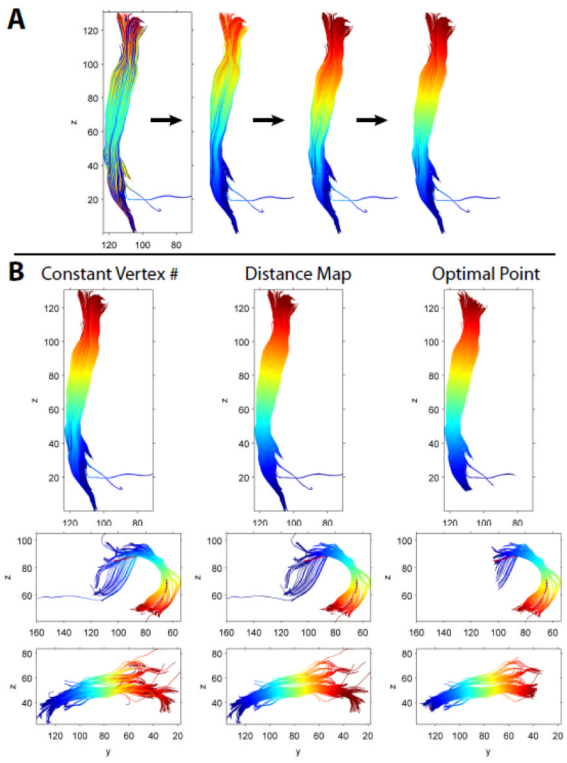

Figure 9. Correspondence plots

Streamlines are colored by vertex index, highlighting which vertices have assigned correspondence and will be grouped together for the analysis (i.e. all vertices with the same dark blue hue will be grouped together, etc.). (A) Left corticospinal tract, after 1) import of raw streamlines, 2) reorientation of streamlines toward a common origin, 3) resampling of streamlines to have the same number of vertices, and 4) automatic prescription of an additional interior point of correspondence. (B) Comparison of 3 different correspondence schemes (columns; Constant Vertex #, Distance Map, Optimal Point), for 3 different tract files (rows; left corticospinal tract, left arcuate fasciculus, left inferior longitudinal fasciculus). The mean tract geometry (i.e., the prototype fiber) is also plotted, and is visible where not obscured by the other fibers.

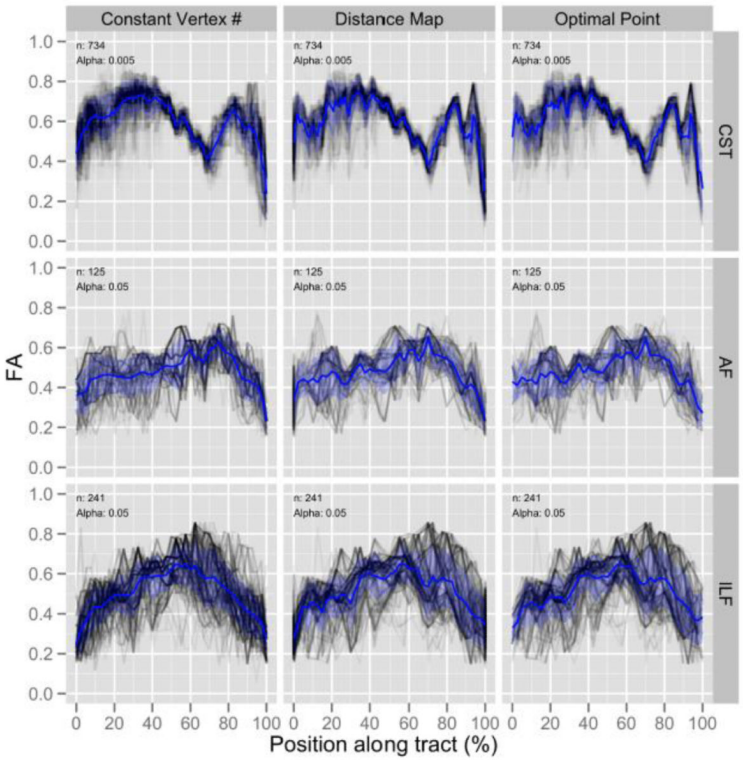

Figure 10. Along-tract plots using different correspondence schemes

FA is plotted versus position from tract origin (similar to Fig. 5). The distribution of individual streamlines is shown in the background (black lines; transparency and slight x-axis jitter used to control overplotting). Overlaid is the along-tract cross-sectional mean FA (blue; ± pointwise standard deviation). Plots are annotated with number of streamlines (n), and transparency value used (alpha). As in Fig. 9, these plots are facetted into a 3×3 grid of different correspondence schemes (columns), and tracts (rows).

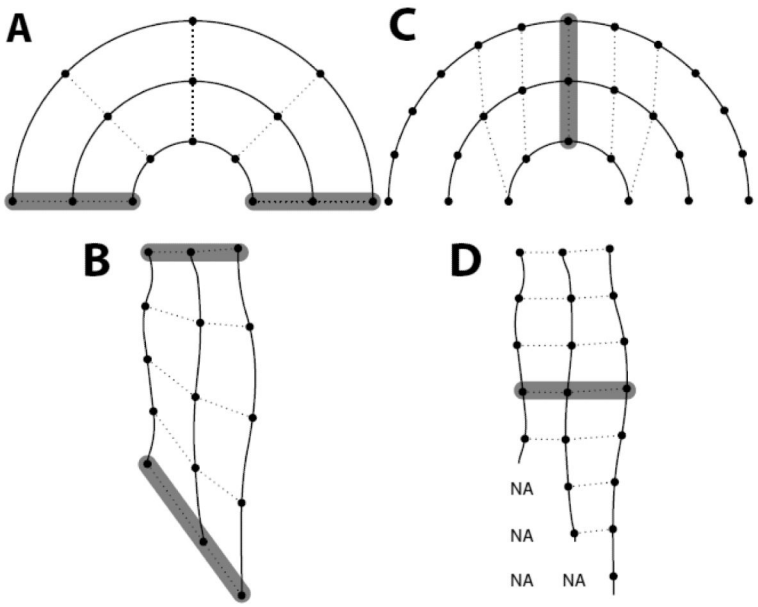

Figure 11. Comparison of resampling strategies

(A,B) Streamlines resampled with a constant number of vertices, but variable spacing, and pinned together at either end (tract origins designated by the gray groupings of vertices). (C,D) Streamlines resampled with variable numbers of vertices, but constant spacing, and pinned together at the midpoint of the mean tract geometry.

Table 1

Single subject tract information and ANOVA results between along-tract and tract-averaged models

Hemisphere, tract origin, number of streamlines, and number of resampled vertices are tabulated for each tract group in the single subject atlas (Fig. 5). The along-tract and tract-averaged linear models were fit to these streamline data, and ANOVA was used to determine if moving to the along-tract approach provided significant increases in explained variance over the tract-averaged form.

Tract	Hemisphere	Origin	Streamlines	Resampled vertices	F	df (numerator, denominator)	*p*-value
Cingulum - cingulate gyrus part	L	Anterior	73	30	48.4	29, 2160	< 2.2e-16
Cingulum - hippocampal part	L	Anterior	71	14	12.4	13, 980	< 2.2e-16
Corticospinal tract	L	Inferior	180	47	138.2	46, 8413	< 2.2e-16
Anterior thalamic radiations	L	Anterior	123	31	43.3	30, 3782	< 2.2e-16
Arcuate fasciculus	L	Frontal	125	40	72.8	39, 4960	< 2.2e-16
Inferior longitudinal fasciculus	L	Anterior	241	41	216.0	40, 9840	< 2.2e-16
Inferior fronto-occipital fasciculus	L	Anterior	99	62	93.6	61, 6076	< 2.2e-16
Uncinate fasciculus	L	Frontal	89	28	48.0	27, 2464	< 2.2e-16
Corpus callosum - forceps major	-	Right	94	64	142.8	63, 5952	< 2.2e-16
Corpus callosum - forceps minor	-	Right	496	41	326.0	40, 20295	< 2.2e-16